

The Heavy Photon Search Experiment at Jefferson Lab

OMAR MORENO¹*Santa Cruz Institute for Particle Physics
University of California, Santa Cruz*

The Heavy Photon Search (HPS) is a new experiment at Jefferson Lab that will search for heavy $U(1)$ vector bosons (heavy photons or dark photons) in the mass range of $20 \text{ MeV}/c^2$ to $1 \text{ GeV}/c^2$. Dark photons in this mass range are theoretically favorable and may mediate dark matter interactions. The dark photon couples to electric charge through kinetic mixing with the photon, allowing its production through a process analogous to bremsstrahlung radiation. HPS will utilize this production mechanism to probe dark photons with relative couplings of $\varepsilon^2 = \alpha'/\alpha \sim 10^{-5}$ to 10^{-10} and search for the e^+e^- or $\mu^+\mu^-$ decay of the dark photon via two signatures (invariant mass and displaced vertex). Using Jefferson Lab's high luminosity electron beam along with a compact, large acceptance forward spectrometer consisting of a silicon vertex tracker, lead tungstate electromagnetic calorimeter and a muon detector, HPS will access hitherto unexplored regions in the mass/coupling space.

PRESENTED AT

DPF 2013

The Meeting of the American Physical Society
Division of Particles and Fields
Santa Cruz, California, August 13–17, 2013

¹On behalf of the Heavy Photon Search Collaboration

1 The Physics Motivating the HPS Experiment

The existence of additional $U(1)$ gauge symmetries of nature are ubiquitous in several Beyond the Standard Model (BSM) theories [1–4]. Indeed, it is natural for the associated gauge boson (heavy photon, dark photon or A') to “kinematically mix” with the Standard Model (SM) photon through the interaction of massive fields [5]. This, in turn, induces an effective coupling of the A' to electric charge, which is suppressed relative to the electron charge by a factor of $\varepsilon \sim 10^{-2} - 10^{-12}$.

The mixing of the photon with the A' offers one of the few, non-gravitational, portals that can be used to search for new “hidden sector” particles. Some theoretical models have envisioned a scenario in which dark matter inhabits the hidden sector, with its interactions mediated via an A' [6–9]. Such models favor an A' mass range on the order of $\sqrt{\varepsilon m_W} \sim \text{MeV-GeV}$, in part because it resolves several recently observed astrophysical phenomena [10]. This includes accounting for the observed excess in the cosmic-ray positron flux [11–13], while remaining in accord with the lack of excess in the anti-proton spectrum [14]. It must also be noted that an A' with a mass in this range could also provide an explanation for the anomalous magnetic moment of the muon [15].

Sensitivity to this hitherto unexplored region of the mass-coupling phase space can be best achieved using high luminosity, fixed target experiments [16]. In such experiments, an electron beam incident on a high Z target will produce dark photons through a process analogous to bremsstrahlung, with the A' subsequently decaying to pairs of fermions. Since the electroproduced A' will carry most of the incident electron beam energy, the opening angle of low mass dark photons will be quite small. Consequently, the A' decay products will be highly boosted, requiring a detector with very forward acceptance that can be placed in close proximity to the target. Maximizing the acceptance will require placing the detector close to the beam plane, which is occupied by the intense flux of multiple Coulomb scattered beam particles and radiative secondaries originating from the target. This establishes a “dead zone” that the detector is unable to encroach in order to avoid extensive radiation damage. Furthermore, the detector must also be operated in vacuum in order to avoid additional background from beam gas interactions. Finally, minimizing the material budget of the active area of the detector is essential to reducing multiple scattering that dominates both the mass and vertex resolutions that determine the experimental sensitivity. These design principles have led to the conception of the HPS detector as shown in Fig. 1. The HPS detector will utilize a compact, large acceptance forward spectrometer consisting of a silicon microstrip tracker (SVT) along with a lead tungstate electromagnetic calorimeter (Ecal), used as the primary trigger, and a muon detector to search for dark photons in the mass range of $20 \text{ MeV}/c^2$ to $1 \text{ GeV}/c^2$ and couplings in the range of $\varepsilon \sim 10^{-2} - 10^{-5}$. What follows is a description of the HPS

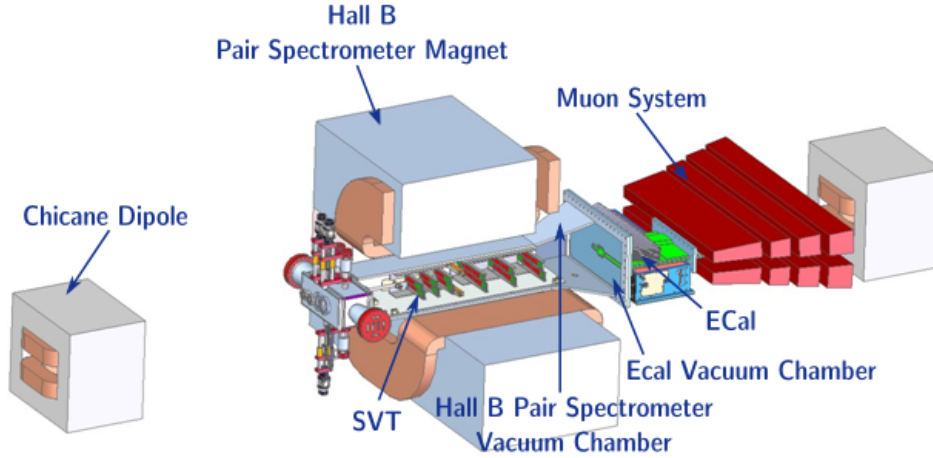


Figure 1: The full HPS detector. It will consist of a six layer silicon microstrip tracker (SVT) installed inside the Hall B pair spectrometer vacuum chamber. A lead tungsten electromagnetic calorimeter (Ecal) will be installed downstream along with a muon system.

experiment* along with discussion of the results from the HPS test run.

2 The HPS Detector

The HPS experiment is proposed to run in experimental Hall B at Jefferson Lab using CEBAF's[†] high luminosity electron beam. CEBAF's continuous duty cycle allows HPS to employ detectors with short live times and rapid readouts in order to diminish backgrounds while maximizing the luminosity. The HPS setup will utilize a three-magnet chicane system with the second dipole, the Hall B pair spectrometer magnet, serving as an analyzing magnet. The target will be placed on the upstream edge of the analyzing magnet and will be 10 cm from the first layer of the SVT, both of which will be housed within the Hall B pair spectrometer vacuum chamber. This setup has been designed to run with beam energies ranging from 1.1 GeV to 6.6 GeV and currents up to 500 nA incident on a thin tungsten target of radiation lengths up to 0.25% X_0 .

The SVT is comprised of six measurement layers, each consisting of a pair of closely-spaced silicon planes as shown in Fig. 2. A stereo angle is introduced between the two planes within each layer allowing for the measurement of both the vertical and bend coordinate of a hit, in turn, enabling full 3D hit reconstruction. The first

*The design of the muon system is a work in progress and will not be described here.

[†]Continuous Electron Beam Accelerator Facility

three layers consist of Hamamatsu Photonics Corporation microstrip sensors and use a stereo angle of 100 mrad. In order to better match the acceptance of the Ecal, the coverage of the last three layers is two sensors wide and use a stereo angle of 50 mrad. In total, the SVT will make use of 36 sensors, which amounts to 23,004 channels (639 channels/sensor). The SVT layout is summarized in Table 1.

The SVT sensors will be continuously read out at 40 MHz using the APV25 readout chip operating in “multi-peak” mode with a 35 ns shaping time. In this mode of operation, six samples of the shaped analog signal are read out per hit. Fitting these samples with a known CR-RC shape then allows for the determination of the initial time of a hit with a resolution of ≈ 2 ns for a $S/N > 25$. A S/N at this level should also result in a spatial resolution of $\approx 6 \mu\text{m}$ [17].

The SVT is split into upper and lower tracking volumes in order to avoid the 15 mrad “dead zone”, putting the active area of the sensors at 1.5 mm from the beam plane. The layers are mounted on upper and lower support structures that are hinged

Layer	1	2	3	4	5	6
z position from target [cm]	10	20	30	50	70	90
Stereo angle [mrad]	100	100	100	50	50	50
Non-bend plane resolution [μm]	≈ 6	≈ 6	≈ 6	≈ 6	≈ 6	≈ 6
Bend-plane resolution [μm]	≈ 60	≈ 60	≈ 60	≈ 120	≈ 120	≈ 120

Table 1: The proposed layout of the SVT.

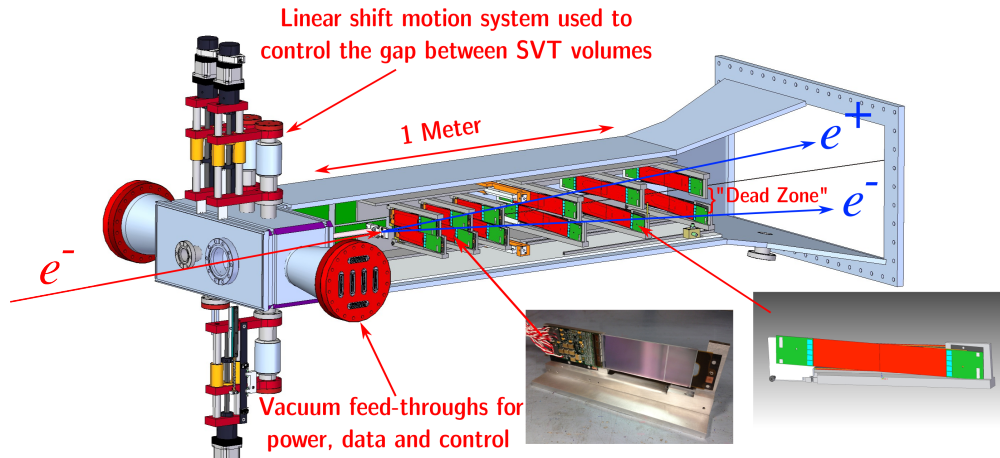


Figure 2: A rendering of the HPS SVT showing the arrangement of the silicon planes inside of the Hall B pair spectrometer vacuum chamber. The silicon sensors are shown in red while the hybrid readout boards are shown in green.

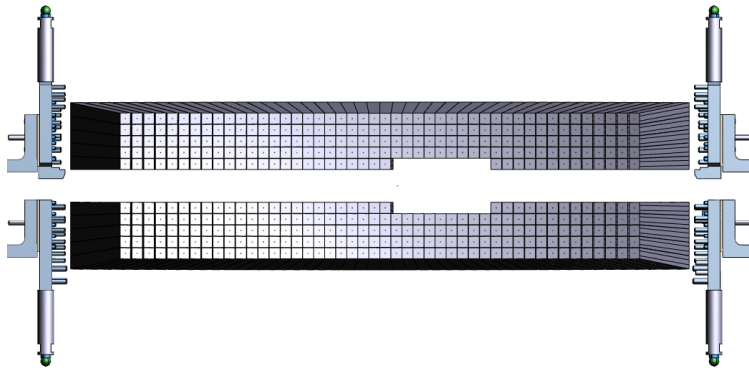


Figure 3: A rendering showing the arrangement of the Ecal crystals. The Ecal is split into upper and lower modules in order to accommodate the “dead zone”. The missing crystals allow a larger opening for the outgoing electron beam.

on the downstream end of the SVT. This allows adjustment of the vertical position of the sensors remotely by a motion control system, in response to experimental conditions.

The Ecal will be used as the primary trigger for the experiment as well as for electron identification. It consists of two volumes (upper and lower), each consisting of five layers of PbWO_4 crystals arranged as shown in Fig. 3. In total, this amounts to 442 crystals. Each of the crystals are read out using avalanche photodiodes at which point each of the output pulses are shaped and preamplified before being digitized by the JLAB FADC250, a 250 MHz flash ADC. Pulse height information along with spatial and timing information is provided to the trigger by the FADC every 8 ns.

3 The HPS Reach

The estimated reach of the HPS experiment at 2σ significance is shown in Fig. 4 along with some existing constraints set by the beam dump experiments E141 [18], E774 [19], Orsay [20] and U70 [21], the collider experiments BaBar [22, 23] and KLOE [24], the fixed target test results reported by APEX [25] and MAMI [26] and the anomalous magnetic moment of the electron [27, 28] and muon [15]. The green band represents the region that an A' can be used to explain the discrepancy between the measured and calculated muon anomalous magnetic moment. The reach calculation assumes running at 1.1 GeV and 2.2 GeV for a week each in 2014 as well as running at 2.2 GeV and 6.6 GeV for two weeks each in 2015. Sensitivity to the upper region is achieved through a bump-hunt search while the lower region utilizes a bump-hunt plus displaced vertex search.

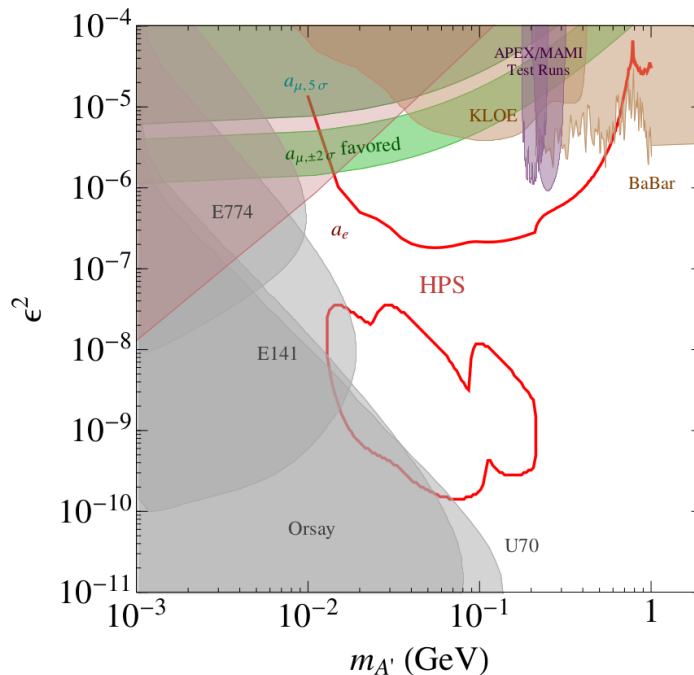


Figure 4: The estimated reach of the HPS experiment at 2σ significance along with existing constraints [15, 18–28]. The reach calculation assumes running at 1.1 GeV and 2.2 GeV for a week each in 2014 and running at 2.2 GeV and 6.6 GeV for three weeks each in 2015.

4 The HPS Test Run

The HPS test run used a simplified version of the full HPS detector in order to demonstrate the technical feasibility of the full HPS apparatus and to confirm that the trigger rates and occupancies encountered during electron-beam running are well understood. The layout of the test run detector is shown in Fig. 5. Other than the absence of the muon system, the central difference to the design of the full detector was the smaller SVT acceptance due to the use of five layers with single sensor coverage. A more thorough description of the test run detector geometry can be found in [29].

The test run detector was designed with the intention of running using an electron beam. However, due to scheduling conflicts at JLab, dedicated electron beam time was not secured. Instead, the experiment ran parasitically using a photon beam with a thin aluminum converter upstream of the detector serving as a target. The conversions originating from the target were used to commission the detector and benchmark the performance of both the test SVT and Ecal. HPS was also granted 8 hours of dedicated photon beam before the CEBAF shutdown. Several runs at currents ranging from 30-90 nA using different converter thicknesses of radiation

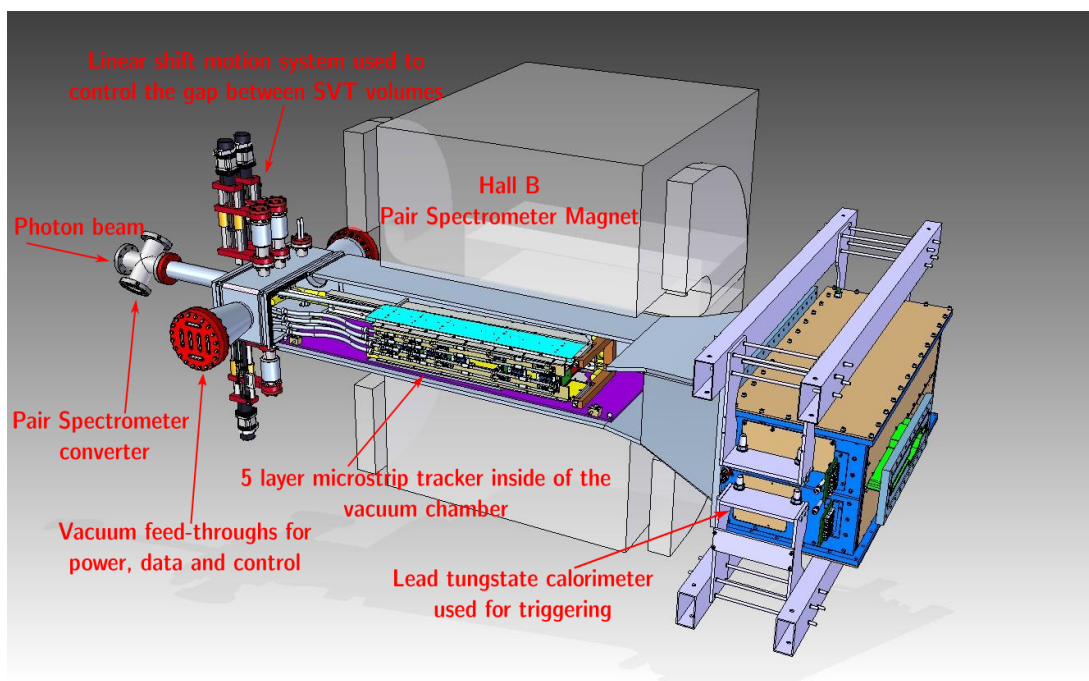


Figure 5: The HPS test run detector. It consist of a five layer silicon microstrip tracker installed inside of the Hall B pair spectrometer vacuum chamber. A PbWO_4 electromagnetic calorimeter was installed downstream and provided the trigger. An aluminum converter upstream of the tracker served as a target.

lengths 1.6%, 0.45% and 0.18% X_0 were taken. The dedicated run was used to measure the normalized trigger rates that established that the backgrounds expected during electron running are well modeled.

Throughout the duration of the test run, $> 97\%$ of the SVT's channels were found to be operational with a signal to noise ratio of ≈ 25.5 . This is enough to achieve a position resolution of $\approx 6 \mu\text{m}$ desired for the full HPS run. The hit time resolution was found to be $\approx 2.6 \text{ ns}$, which is enough to aid in the reduction of background due to pileup. The single hit efficiency was also shown to exceed 98% for good channels while tracks were reconstructed with very high efficiency and purity. Finally, the survey-based alignment of the SVT was shown to be adequate enough to allow the use of track-based alignment.

The Ecal performed similarly well with 87% of the crystals found to be operational. The trigger functioned as designed and tests showed that it can achieve trigger rates greater than 100 kHz.

The requirement that the SVT be as close to the beam plane as possible creates one of the key challenges for the HPS experiment. Simulations have shown that the dominant source of occupancy for the HPS experiment comes from beam electrons

that have multiple Coulomb scattered in the target into large angles. However, the multiple Coulomb scattering rate at large angles is overestimated by Geant4 by a factor of two when compared to EGS5 [29]. It is then crucial to verify that the correct model of multiple Coulomb scattering is being used by the simulation in order to establish that HPS can run at the proposed electron beam currents.

The angular distribution of the conversions produced in the aluminum target are a convolution of both the pair production angle and the multiple Coulomb scattering of the electron-positron pairs. It is then possible to confirm the model of multiple Coulomb scattering by using the data taken during the dedicated photon run. Comparing the measured angular distribution for each of the converter thicknesses to those from simulation verifies that EGS5 predicts the correct distributions while Geant4 overestimates the rates. In fact, the normalized trigger rates as simulated by EGS5 agree with the test run data to within 10% as shown in Fig. 6. This verifies the EGS5 model of multiple Coulomb scattering and provides confidence that the beam backgrounds expected during the full run are as simulated.

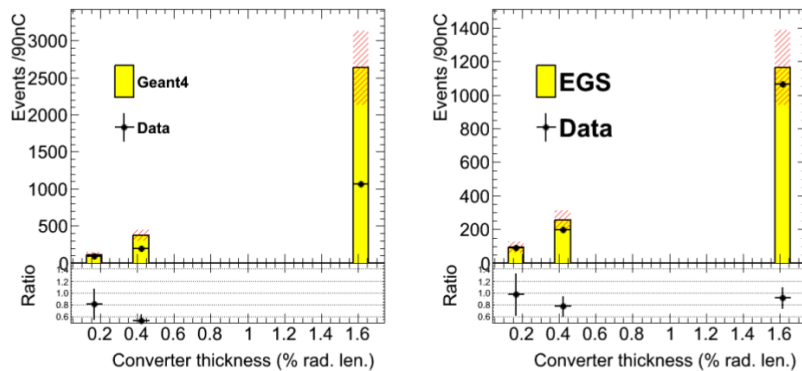


Figure 6: The normalized trigger rates as a function of converter thickness. The trigger rates simulated by EGS5 agree with the test run data to within 10%.

5 Conclusion

The HPS test run successfully demonstrated that the design of the full detector is technically feasible. Specifically, the SVT was able to demonstrate that the signal to noise, timing and position resolutions were as expected while the Ecal trigger functioned as designed. In addition, the EGS5 model of multiple Coulomb was verified. After the test run, a proposal for the full HPS experiment was submitted to the Department of Energy and has now been approved. Construction of the full experiment is now underway and should be ready for installation and data taking in the Fall of 2014.

References

- [1] M. Goodsell and A. Ringwald, Fortsch. Phys. **58**, 716 (2010) [arXiv:1002.1840 [hep-th]].
- [2] P. Candelas, G. T. Horowitz, A. Strominger and E. Witten, Nucl. Phys. B **258**, 46 (1985).
- [3] S. Andreas, M. D. Goodsell and A. Ringwald, Phys. Rev. D **87**, 025007 (2013) [arXiv:1109.2869 [hep-ph]].
- [4] J. Jaeckel and A. Ringwald, Ann. Rev. Nucl. Part. Sci. **60**, 405 (2010) [arXiv:1002.0329 [hep-ph]].
- [5] B. Holdom, Phys. Lett. B **166**, 196 (1986).
- [6] N. Arkani-Hamed, D. P. Finkbeiner, T. R. Slatyer and N. Weiner, Phys. Rev. D **79**, 015014 (2009) [arXiv:0810.0713 [hep-ph]].
- [7] M. Pospelov and A. Ritz, Phys. Lett. B **671**, 391 (2009) [arXiv:0810.1502 [hep-ph]].
- [8] C. Cheung, J. T. Ruderman, L. -T. Wang and I. Yavin, Phys. Rev. D **80**, 035008 (2009) [arXiv:0902.3246 [hep-ph]].
- [9] N. Arkani-Hamed and N. Weiner, JHEP **0812**, 104 (2008) [arXiv:0810.0714 [hep-ph]].
- [10] R. Essig, J. Kaplan, P. Schuster and N. Toro, [arXiv:1004.0691 [hep-ph]].
- [11] O. Adriani *et al.* [PAMELA Collaboration], Nature **458**, 607 (2009) [arXiv:0810.4995 [astro-ph]].
- [12] M. Ackermann *et al.* [Fermi LAT Collaboration], Phys. Rev. Lett. **108**, 011103 (2012) [arXiv:1109.0521 [astro-ph.HE]].
- [13] M. Aguilar *et al.* [AMS Collaboration], Phys. Rev. Lett. **110**, no. 14, 141102 (2013).
- [14] O. Adriani *et al.* [PAMELA Collaboration], Phys. Rev. Lett. **105**, 121101 (2010) [arXiv:1007.0821 [astro-ph.HE]].
- [15] M. Pospelov, Phys. Rev. D **80**, 095002 (2009) [arXiv:0811.1030 [hep-ph]].
- [16] J. D. Bjorken, R. Essig, P. Schuster and N. Toro, Phys. Rev. D **80**, 075018 (2009) [arXiv:0906.0580 [hep-ph]].

- [17] P. Azzi, N. Bacchetta, G. Martignon, M. Menguzzato, A. Ribon and R. Rosin
CDF Internal Note CDF/DOC/TRACKING/CDFR/5080 (1999)
- [18] E. M. Riordan, M. W. Krasny, K. Lang, P. De Barbaro, A. Bodek, S. Dasu,
N. Varelas and X. Wang *et al.*, Phys. Rev. Lett. **59**, 755 (1987).
- [19] A. Bross, M. Crisler, S. H. Pordes, J. Volk, S. Errede and J. Wrbanek, Phys.
Rev. Lett. **67**, 2942 (1991).
- [20] S. Andreas, C. Niebuhr and A. Ringwald, Phys. Rev. D **86**, 095019 (2012)
[arXiv:1209.6083 [hep-ph]].
- [21] J. Blumlein and J. Brunner, Phys. Lett. B **701**, 155 (2011) [arXiv:1104.2747
[hep-ex]].
- [22] B. Aubert *et al.* [BaBar Collaboration], Phys. Rev. Lett. **103** (2009) 081803
[arXiv:0905.4539 [hep-ex]].
- [23] R. Essig, P. Schuster, N. Toro and B. Wojtsekhowski, JHEP **1102**, 009 (2011)
[arXiv:1001.2557 [hep-ph]].
- [24] D. Babusci *et al.* [KLOE-2 Collaboration], Phys. Lett. B **720** (2013) 111
[arXiv:1210.3927 [hep-ex]].
- [25] S. Abrahamyan *et al.* [APEX Collaboration], Phys. Rev. Lett. **107**, 191804 (2011)
[arXiv:1108.2750 [hep-ex], arXiv:1108.2750 [hep-ex]].
- [26] H. Merkel *et al.* [A1 Collaboration], Phys. Rev. Lett. **106**, 251802 (2011)
[arXiv:1101.4091 [nucl-ex]].
- [27] M. Endo, K. Hamaguchi and G. Mishima, Phys. Rev. D **86**, 095029 (2012)
[arXiv:1209.2558 [hep-ph]].
- [28] H. Davoudiasl, H. -S. Lee and W. J. Marciano, Phys. Rev. D **86**, 095009 (2012)
[arXiv:1208.2973 [hep-ph]].
- [29] P. Hansson Adrian *et al.* [HPS Collaboration], Heavy Photon Search
Experiment at Jefferson Laboratory: Proposal for 2014-2015 run,
<https://confluence.slac.stanford.edu/display/hpsg/HPS+Proposals>